Generation of Radiation Null for the HMSIW Leaky-Wave Antenna

Xuyang Chen, Zheng Li, *Member, IEEE*, He Song, and Junhong Wang, *Senior Member, IEEE*

***Abstract*—A new design of half-mode substrate integrated waveguide leaky-wave antenna with radiation null in the radiation pattern is proposed in this letter. The radiation null is realized by controlling the leakage constant of the effective radiation sections (ERSs). By changing the vias position and extending width of substrate at the locations of the ERSs for the prescribed angle, the null region can occur in any desired direction. In this way a null region with depth 36.2 dB around $\theta = -96^\circ$ at 9 GHz is achieved, and at the same time the main beam is almost not affected. A tapered microstrip line with shaped single-stub tuning is used for good impedance matching with the antenna. The advantage of this design is that only simple modification of structure is needed to achieve good result of radiation null.**

***Index Terms*—Effective radiation section (ERS), half-mode substrate integrated waveguide (HMSIW), leaky-wave antenna (LWA), radiation null.**

I. Introduction

THE wireless communication technology has promoted rapid development of antenna technologies, among which the leaky-wave antenna (LWA) is a hot research topic due to its good abilities of frequency scanning and high directivity [1]. The emergence of new technology, such as the substrate integrated waveguide (SIW) [2], [3], provides new opportunities for the development of LWAs. The SIW has many advantages, such as low loss, low cost, easy fabrication and integration, and high frequency applicability. The half-mode substrate integrated waveguide (HMSIW) can be implemented by splitting the SIW into two parts along the symmetric plane, which is equivalent to a magnetic wall [4], [5]. The width of HMSIW is merely half of the full-mode SIW and can support the TE0.5,0 mode. Then, many studies on the LWAs using the HMSIW structure are presented. In [6], an LWA with wide bandwidth and quasi-omnidirectional radiation pattern is implemented using HMSIW at Ka-band. In [7], a frequency scanning antenna based on HMSIW is presented with the dynamical change of the polarization state. A horizontally polarized HMSIW antenna using a direct transition from coaxial connector is proposed in [8], exhibiting a wide bandwidth and omnidirectional radiation pattern.

Manuscript received July 12, 2017; revised August 3, 2017; accepted August 12, 2017. Date of publication August 17, 2017; date of current version September 25, 2017. This work was supported in part by the National Nature Science Foundation of China under Grant 61331002, and in part by the National Program on Key Basic Research Project under Grant 2013CB328903. *(Corresponding Author: Zheng Li.)*

The authors are with the Key Laboratory of All Optical Network and Advanced Telecommunication Network of Ministry of Education, and the Institute of Lightwave Technology, Beijing Jiaotong University, Beijing 100044, China (e-mail: 15120001@bjtu.edu.cn; lizheng@bjtu.edu.cn; 15120025@bjtu.edu.cn; wangjunh@bjtu.edu.cn).

Color versions of one or more of the figures in this letter are available online at http://ieeexplore.ieee.org.

Digital Object Identifier 10.1109/LAWP.2017.2741099

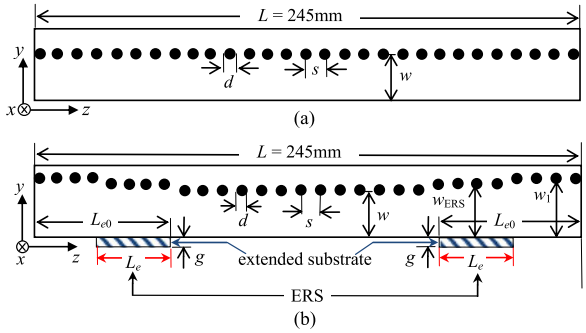

Fig. 1. Configurations of the two antennas. (a) Conventional HMSIW LWA. (b) Proposed LWA.

In some communication occasions, radiation null may be needed in some specific angular regions for reducing interference or undesired radiation. There have been many studies on the pattern synthesis methods and optimization algorithms for array antennas to generate radiation nulls [9]–[12]. However, there is little research on the null generation for LWAs. In [13], a method based on iterative fast Fourier transform technique is proposed to generate radiation null for LWA. The leakage constant and phase constant along the aperture are controlled simultaneously by continuously tapering the slot, and hence the radiation null can be obtained. In [14], a method of lossy transmission line model for the nonuniform LWAs is proposed, and a method for radiation pattern synthesis is presented based on global optimization. This method shows good results in the radiation null generation and has high flexibility in design. The concept of effective radiation sections (ERSs) provides a new insight for traveling-wave radiation mechanism [15]. It demonstrates that the far-field radiation in a given direction can be approximately calculated by the radiation from ERSs since the radiation fields from the other sections are cancelled by each other. The ERSs can be adopted in the pattern synthesis of LWAs to realize radiation null or low sidelobe level, and a preliminary study is given in [16]. In this letter, the method of generating null region for LWA is studied in detail. Using this method, a new design of HMSIW LWA is realized with radiation null in desired angular range.

II. Configuration and Theory

The configurations of the conventional HMSIW LWA and the proposed design are shown in Fig. 1 for comparison. The antennas are constructed in Rogers RT5880 substrate with dielectric constant $\varepsilon_r = 2.2$ and thickness $h = 0.787$ mm. The total aperture length is $L = 245$ mm, and the width of the HMSIW

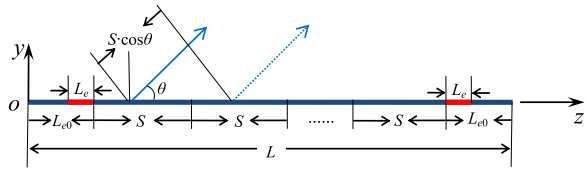

Fig. 2. Magnetic-current line-source model.

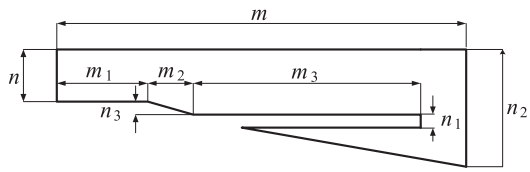

Fig. 3. Configuration of the feeding line. ($m = 21$ mm, $n = 2.46$ mm, $m_1 = 5$ mm, $m_2 = 1.64$ mm, $m_3 = 11.37$ mm, $n_1 = 0.3$ mm, $n_2 = 4.43$ mm, $n_3 = 0.2$ mm).

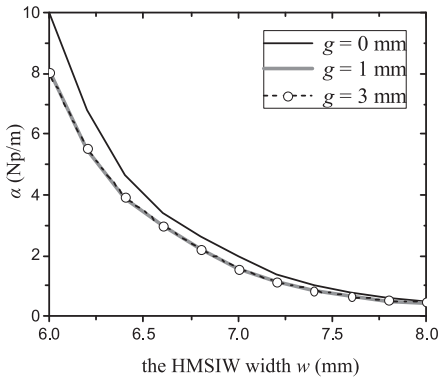

Fig. 4. Relationship between α and w, g at 9 GHz.

antenna is $w = 6.4$ mm. The diameter of each via is $d = 1$ mm, and the spacing between adjacent vias is $s = 2$ mm.

The conventional HMSIW LWA is shown in Fig. 1(a), and the radiation aperture can be approximately equivalent to a magnetic-current line-source model, as shown in Fig. 2. In this figure, the ERSs are marked in red color, and L_e and L_{e0} represent the length and location of ERSs, respectively. The ERSs can be calculated using the method in [15]. The power along the LWA can be expressed as $P(z) = P(0)\exp(-2\alpha z)$, where $P(0)$ is the initial power, and then we can get the power radiated per unit length as $-\frac{dP(z)}{dz} = 2\alpha P(z) = 2\alpha P(0)\exp(-2\alpha z)$. Thus, the radiated E-field strength is proportional to $\sqrt{|\frac{dP(z)}{dz}|} = \sqrt{\alpha P(0)}\exp(-\alpha z)$, and the radiation of the whole line source can be obtained by the following integration:

$$f(\theta) = A\sqrt{\alpha(z)} \cdot \sin\theta \cdot \int_0^L \exp(-(j\beta + \alpha(z))z + jk_0 y\cos\theta)dz\sqrt{2} \quad (1)$$

in which β is the phase constant, θ is the observation angle, and A is a constant coefficient.

Assume that α_{ERS} and α are the leakage constants for ERSs and the rest parts of the structure, respectively. Then, in this letter, a new formula describing the far-field calculation of the line-source model can be achieved as follows:

$$\begin{aligned} f\left(\theta\right) = {} & A\sqrt{\alpha_{\text{ERS}}}\sin\theta \cdot \left[\left(\int_{Le0-Le}^{Le0} + \int_{L-Le0}^{L-Le0+Le}\right)\right. \\ & \left.\times \exp(-(j\beta + \alpha_{\text{ERS}})z + jk_0 y\cos\theta)dz\right] \\ & + A\sqrt{\alpha}\sin\theta \cdot \left[\left(\int_0^{Le0-Le} + \int_{L-Le0+Le}^{L} + \int_{Le0}^{L-Le0}\right)\right. \\ & \left.\times \exp(-(j\beta + \alpha)z + jk_0 y\cos\theta)dz\right]. \end{aligned} \quad (2)$$

Equation (2) demonstrates that the total far field consists of two parts: The first term represents the radiation from the ERSs, which contributes the most to the far field; the second term represents the radiation from the rest of the line source, which has little contribution to the far field since their radiations can be cancelled by each other according to the analysis in [15]. Therefore, the total far field $f(\theta)$ can be approximately determined only by the ERSs. Different leakage constants are used for the ERSs and other sections, which have more accurate physical meaning and are closely related with radiation characteristic of the actual structure. So if we can find a way to control the value of α_{ERS} (the leakage constant of the ERSs), the radiation strength by the ERSs can be controlled, and hence a radiation null can be generated in a desired direction in the radiation pattern of the line-source model.

For a practical HMSIW LWA, by changing the structure corresponding to the ERSs (including the vias positions and the proper extension of the substrate), as shown in Fig. 1(b), the radiation strength of ERSs can be suppressed, and a null region is expected in a desired angular range. A tapered microstrip line is designed as the feeding structure as shown in Fig. 3. A shaped single-stub tuning is employed for impedance matching between the antenna and feeding line [17].

III. Results and Discussion

Assume that the conductor is perfect electric conductor and the substrate has no dielectric loss. Then, the leakage constant is approximately equal to the attenuation constant along the HMSIW and can be calculated by $\alpha = -\ln|S_{21}|/L$. As stated in Section II, the leakage constant α_{ERS} at the locations of ERSs can be controlled by changing the vias positions and extending the substrate, that is, changing w_{ERS} and g in Fig. 1(b). Since the relationship between α_{ERS}, w_{ERS}, and g cannot be obtained directly for the structure in Fig. 1(b), a conventional HMSIW with uniform structure shown in Fig. 1(a) (unchanged w and g along the whole structure) is simulated, and the result of α is shown in Fig. 4. According to the relationship in Fig. 4, we just need to change w_{ERS} and g only at the location of ERS to realize a desired α_{ERS}. From Fig. 4, it can be seen that at 9 GHz the value of α decreases significantly when the width w increases from 6.0 to 8.0 mm. Extending the width g can also decrease α dramatically when w is small, but this effect becomes obscure when g is larger than 1 mm according to this figure. It is inferred that the parameter w has a stronger effect on the adjustment of α than the parameter g. Consequently, in order to achieve a required α_{ERS}, the specific structural parameters w_{ERS} and g can be determined from Fig. 4, and hence, the radiation strength of the ERSs can be controlled. The structural parameters of the conventional HMSIW are set as $w = 6.4$ mm and $g = 0$ mm, and we have $\alpha = 4.64$ Np/m. In addition, the phase constant β can be extracted from the aperture field obtained by the full-wave simulation, and we can get $\beta = 126.13$ rad/m.

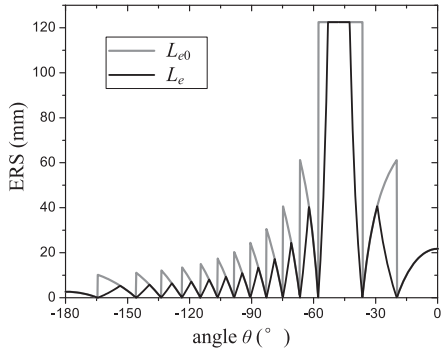

Fig. 5. Length and location of the ERSs as function of angle φ at 9 GHz.

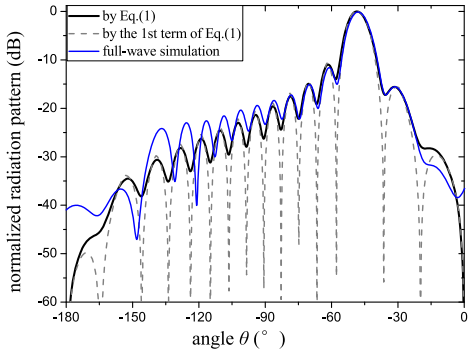

Fig. 6. Normalized radiation patterns of the magnetic-current line-source model and by the full-wave simulation at 9 GHz.

Substituting $\alpha = 4.64\,\mathrm{Np/m}$ and $\beta = 126.13\,\mathrm{rad/m}$ into the magnetic-current line-source model, the radiation pattern of the line source can be calculated, and hence, the radiation property of the HMSIW LWA can be studied in a theoretical way. First, we have to calculate the ERSs of the line-source model. Using (4) in [15], the distribution of the ERSs as function of the observation angle φ at 9 GHz can be achieved, as shown in Fig. 5. From Fig. 5, we can obtain all the information including the length and location of ERSs for each angle. Using the ERSs, the normalized radiation pattern generated only by the ERSs can be calculated by the first term in (2), and the result (grey curve) is given in Fig. 6. The result of the whole line source obtained by the whole (2) is also given for comparison (black curve). It can be seen that these two curves match well with each other except in the null depth, demonstrating that the far-field radiation is mainly determined by the ERSs [the first term in (2)], while the residual sections [the second term in (2)] have little contribution to the total radiation. The full-wave simulation result of the conventional HMSIW LWA (blue curve) is obtained by CST, showing good agreement with the line source result on the main beam and the sidelobes near the main beam. This demonstrates that the line-source model is a valid equivalence for the practical antenna, and the ERS method is suitable for the analysis of this antenna.

Assume that the angular range of radiation null is desired to be around $\theta = -96^\circ$. From Fig. 5, we can get the location and length of the ERSs in $\theta = -96^\circ$ as $L_{e0} = 14.79\,\mathrm{mm}$ and $L_e = 6.76\,\mathrm{mm}$. By (2), the normalized radiation patterns of the line-source model at 9 GHz are obtained when α_{ERS} is changed, as shown in Fig. 7. It can be seen that when α_{ERS} decreases ($\alpha_{\mathrm{ERS}} \in [0, \alpha]$), the radiation strength in the angular range around $\theta = -96^\circ$ is suppressed, and an obvious null region appears. In addition, the main beam is not affected obviously.

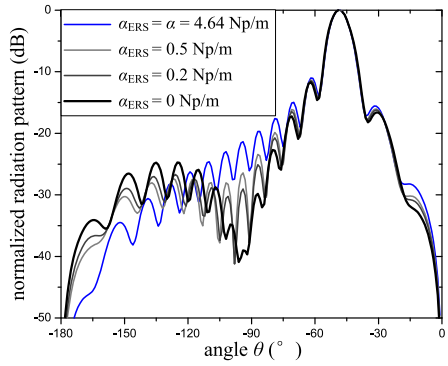

Fig. 7. Normalized radiation patterns of the magnetic-current line-source model when α_{ERS} varies.

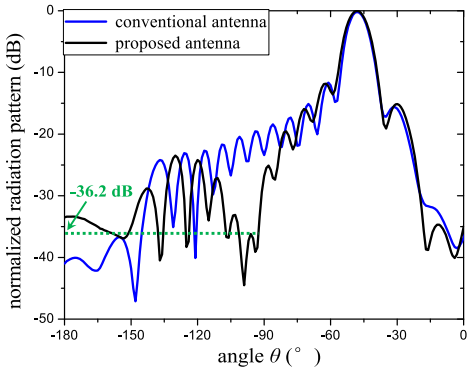

Fig. 8. Simulated radiation patterns for the proposed antenna and the conventional antenna.

For a practical HMSIW LWA, adjustment of the α_{ERS} can be implemented by changing the vias position and extending the substrate at the locations of the ERSs simultaneously, as shown in Fig. 1(b). The waveguide width corresponding to the ERSs is $w_{\mathrm{ERS}} = 7.8\,\mathrm{mm}$. After optimization, the width g is set to be 2.9 mm because the structural mutation at the location of the extended substrate has an effect on the value of α_{ERS}, which is not exactly equal to the value in Fig. 4. In addition, S_{11} might deteriorate seriously due to the change of vias, and also the reflected lobe level might be high. To solve this problem, the width w_1 close to the terminal of the antenna is increased a little to be $w_1 = 8.5\,\mathrm{mm}$ for the purpose of good matching between the HMSIW and the feeding line and lower reflected lobe level.

The radiation patterns of gain in H-plane at 9 GHz for the proposed antenna and the conventional antenna are given in Fig. 8 for comparison. An obvious null can be observed around the prescribed angle $\theta = -96^\circ$, and the maximum null depth is –36.2 dB. The gain of the conventional LWA is 11.3 dBi, and the gain of the proposed antenna is 11.1 dBi. The antenna efficiency is around 83% for both the conventional antenna and the proposed antenna. This demonstrates that the proposed method for generating radiation null has little effect on the gain and antenna efficiency.

Both the conventional antenna and the designed antenna are fabricated, as shown in Fig. 9. The measured radiation patterns are given in Fig. 10. It can be observed that a null region occurs in the angular range from –118° to –94°, and the maximum null depth is –26.6 dB. The measured gain for the two fabricated antennas is about 9 dBi. Fig. 10 is not so good as the simulated result in Fig. 8, probably due to machining, soldering, and

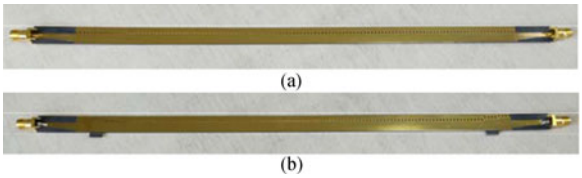

Fig. 9. Photographs of the fabricated antennas. (a) Conventional antenna. (b) Proposed antenna.

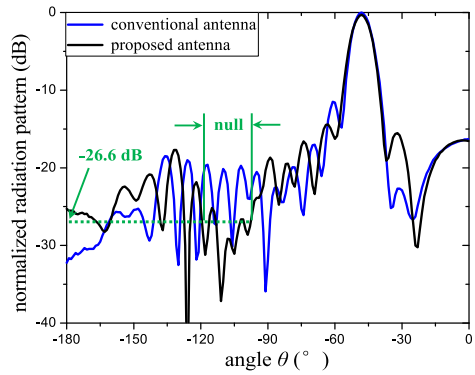

Fig. 10. Measured radiation patterns for the proposed antenna and the conventional antennas.

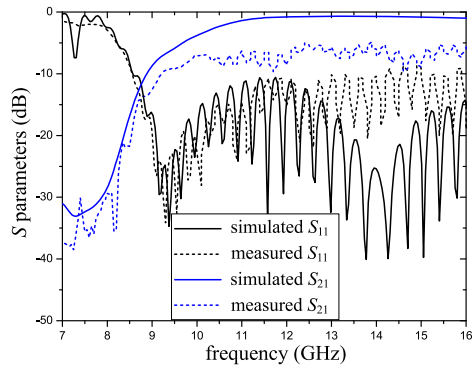

Fig. 11. Comparison of the simulated and measured S-parameters of the proposed antennas.

experimental errors (especially for the measurement accuracy of the lobes with low level). Nevertheless, the validity of the method has been verified. Using the proposed method, null can be introduced in the radiation pattern in other desired angular ranges.

The simulated and measured S-parameters for the antennas are shown in Fig. 11. The frequency band starts from 8.58 GHz for both the simulated and measured results. There are some differences on the values of S_{21}, which is probably caused by fabrication errors, soldering of connectors, and spurious radiations from the discontinuities of the feeding structure.

IV. Conclusion

An HMSIW LWA with radiation null in its radiation pattern is designed in this letter. The method of ERSs is employed to generate null region in any prescribed direction. A null depth of 36.2 dB in $\theta = -96^\circ$ is achieved in the radiation pattern at 9 GHz. At the same time this method has almost no influence on the main beam. To obtain a better impedance matching with the antenna, a tapered microstrip line with single-stub tuning is employed. This method of generating null region has the advantage of simple change of structure and good result of radiation null.

Acknowledgment

The authors would like to acknowledge measurement help by the EM lab in the School of Information Engineering at the Communication University of China.

References

[1] A. A. Oliner and D. R. Jackson, "Leaky-wave antennas," in *Antenna Engineering Handbook*, J. L. Volakis, Ed., 4th ed. New York, NY, USA: McGraw-Hill, 2007.

[2] D. Deslandes and K. Wu, "Integrated microstrip and rectangular waveguide in planar form," *IEEE Microw. Wireless Compon. Lett.*, vol. 11, no. 2, pp. 68–70, Feb. 2001.

[3] Y. Cassivi, L. Perregrini, P. Arcioni, M. Bressan, K. Wu, and G. Conciauro, "Dispersion characteristics of substrate integrated rectangular waveguide," *IEEE Microw. Wireless Compon. Lett.*, vol. 12, no. 9, pp. 333–335, Sep. 2002.

[4] B. Liu, W. Hong, Y. Zhang, J. X. Chen, and K. Wu, "Half-mode substrate integrated waveguide (HMSIW) double-slot coupler," *Electron. Lett.*, vol. 43, no. 2, pp. 113–114, Jan. 2007.

[5] Y. J. Cheng, W. Hong, and K. Wu, "Half mode substrate integrated waveguide (HMSIW) directional filter," *IEEE Microw. Wireless Compon. Lett.*, vol. 17, no. 7, pp. 504–506, Jul. 2007.

[6] J. Xu, W. Hong, H. Tang, Z. Kuai, and K. Wu, "Half-mode substrate integrated waveguide (HMSIW) leaky-wave antenna for millimeter-wave applications," *IEEE Antennas Wireless Propag. Lett.*, vol. 7, pp. 85–88, 2008.

[7] Y. J. Cheng, W. Hong, and K. Wu, "Millimeter-wave half mode substrate integrated waveguide frequency scanning antenna with quadri-polarization," *IEEE Trans. Antennas Propag.*, vol. 58, no. 6, pp. 1848–1855, Jun. 2010.

[8] N. Nguyen-Trong, T. Kaufmann, and C. Fumeaux, "A wideband omnidirectional horizontally polarized traveling-wave antenna based on half-mode substrate integrated waveguide," *IEEE Antennas Wireless Propag. Lett.*, vol. 12, pp. 682–685, 2013.

[9] R. Ghayoula, N. Fadlallah, A. Gharsallah, and M. Rammal, "Phase-only adaptive nulling with neural networks for antenna array synthesis," *Microw. Antennas Propag.*, vol. 3, no. 1, pp. 154–163, Feb. 2009.

[10] H. Wu, C. Liu, and Y. Dai, "Adaptive pattern nulling design of linear array antenna by phase perturbations using invasive weed optimization algorithm," in *Proc. 2013 3rd Int. Conf. IEEE Inf. Sci. Technol.*, 2013, pp. 1372–1374.

[11] Y. J. Lee, J. W. Seo, J. K. Ha, and D. C. Park, "Null steering of linear phased array antenna using genetic algorithm," in *Proc. 2009 Asia Pacific Microw Conf.*, 2009, pp. 2726–2729.

[12] H. Steyskal, R. Shore, and R. Haupt, "Methods for null control and their effects on the radiation pattern," *IEEE Trans. Antennas Propag.*, vol. AP-34, no. 3, pp. 404–409, Mar. 1986.

[13] J. L. Gomez-Tornero, A. J. Martinez-Ros, and R. Verdu-Monedero, "FFT synthesis of radiation patterns with wide nulls using tapered leaky-wave antennas," *IEEE Antennas Wireless Propag. Lett.*, vol. 9, pp. 518–521, 2010.

[14] N. Nguyen-Trong, L. Hall, and C. Fumeaux, "Transmission-line model of nonuniform leaky-wave antennas," *IEEE Trans. Antennas Propag.*, vol. 64, no. 3, pp. 883–893, Mar. 2016.

[15] Z. Li, J. H. Wang, Z. Zhang, and M. E. Chen, "Far field computation of the traveling wave structures and a new approach for suppressing the side lobe levels," *IEEE Trans. Antennas Propag.*, vol. 61, no. 4, pp. 2308–2312, Apr. 2013.

[16] Z. Li, J. H. Wang, J. J. Duan, Z. Zhang, and M. E. Chen, "New approach of radiation pattern control for leaky-wave antennas based on the effective radiation sections," *IEEE Trans. Antennas Propag.*, vol. 63, no. 7, pp. 2867–2878, Jul. 2015.

[17] C. Jin and A. Alphones, "Leaky-wave radiation behavior from a double periodic composite right/left-handed substrate integrated waveguide," *IEEE Trans. Antennas Propag.*, vol. 60, no. 4, pp. 1727–1735, Apr. 2012.